Structural Basis for the Altered Activity of Gly794 Variants of *Escherichia coli* β-Galactosidase†

Douglas H. Juers,‡ Shamina Hakda,§ Brian W. Matthews,*,‡ and Reuben E. Huber§

Howard Hughes Medical Institute, Institute of Molecular Biology, and Department of Physics, 1229, University of Oregon, Eugene, Oregon 97403-1229, and Division of Biochemistry, Faculty of Science, University of Calgary, Calgary, Alberta T2N 1N4, Canada

Received August 21, 2003

ABSTRACT: The open−closed conformational switch in the active site of *Escherichia coli* β-galactosidase was studied by X-ray crystallography and enzyme kinetics. Replacement of Gly794 by alanine causes the apoenzyme to adopt the closed rather than the open conformation. Binding of the competitive inhibitor isopropyl thio-β-D-galactoside (IPTG) requires the mutant enzyme to adopt its less favored open conformation, weakening affinity relative to wild type. In contrast, transition-state inhibitors bind to the enzyme in the closed conformation, which is favored for the mutant, and display increased affinity relative to wild type. Changes in affinity suggest that the free energy difference between the closed and open forms is 1−2 kcal/mol. By favoring the closed conformation, the substitution moves the resting state of the enzyme along the reaction coordinate relative to the native enzyme and destabilizes the ground state relative to the first transition state. The result is that the rate constant for galactosylation is increased but degalactosylation is slower. The covalent intermediate may be better stabilized than the second transition state. The substitution also results in better binding of glucose to both the free and the galactosylated enzyme. However, transgalactosylation with glucose to produce allolactose (the inducer of the *lac* operon) is slower with the mutant than with the native enzyme. This suggests either that the glucose is misaligned for the reaction or that the galactosylated enzyme with glucose bound is stabilized relative to the transition state for transgalactosylation.

β-Galactosidase (β-D-galactoside galactohydrolase, EC 3.2.1.23) from *Escherichia coli* is a well-known enzyme with a rich history in molecular biology and biochemistry (*1*−*4*). The enzyme is commonly used as a "reporter" for molecular biology. The amino acid (*5*) and nucleotide (*6*) sequences of the enzyme have been determined. The enzyme is a tetramer, and each identical monomer (116 353 Da, 1023 amino acid residues) functions independently (*7*). Mg^{2+} or Mn^{2+} (*8, 9*) and Na^+ or K^+ (*10*) are required for full catalytic efficiency. The three-dimensional structure of the enzyme is known (*11, 12*) and shows that the active site is in a deep pocket within a distorted triosephosphate isomerase (TIM) barrel. The structures of several inhibitor complexes with the enzyme have been determined (*13*).

β-Galactosidase catalyzes hydrolytic and transgalactosidic reactions with β-D-galactosides (*14*) in a double displacement reaction involving a covalent galactosyl-enzyme intermediate. Recent studies have suggested that there are two binding modes for ligands to the enzyme. Galactosides (PTG, IPTG, PETG, 2-F-lactose)[1] bind in a "shallow" mode and "stack" with Trp999 (*13, 15*). Transition-state analogue inhibitors (D-galactonolactone, D-galactotetrazole, L-ribose), the covalent intermediate, and D-galactose bind in a "deep" mode, further from Trp999 and close to Trp568. Deep mode binding is often accompanied by an enzyme conformational switch (Figure 1) in which the loop from Gly794 to Pro803 swings toward the active site with residue shifts up to 9 Å (*13*).

Although Gly794 is quite far from the catalytic residues (about 15 Å from both the nucleophile, Glu537, and the acid/base, Glu461), it appears to play a significant role in activity. Its importance was first identified in a screen looking for *lacZ* variants active against lactobionic acid, which is normally a very poor substrate for β-galactosidase (*16*). Subsequent biochemical study of Gly794 variants has shown that they often have increased activity with slow substrates such as PNPG and the physiological ligand, lactose (*17*). This occurs via an increase of the rate for the first step, galactosylation (k_2). There is also a decrease in the rate of the second step, degalactosylation (k_3), but if this degalactosylation rate is greater than the galactosylation rate, the overall rate will increase. That variants at position 794 have increased activity against the natural substrate, lactose, is perhaps a little perplexing, as one may wonder why nature has not used these variants.

Gly794 is also interesting structurally because it appears to act somewhat as a "hinge" in the 794−803 loop swing

† This work was supported, in part, by NIH Grant GM20066 to B.W.M. and National Science and Engineering Research Council (Canada) Grant 4691 to R.E.H.

‡ University of Oregon.

§ University of Calgary.

[1] Abbreviations: CE, capillary electrophoresis; IPTG, isopropyl thio-β-D-galactoside; PTG, phenyl thio-β-D-galactoside; PETG, phenylethyl thio-β-D-galactoside; oNP, *o*-nitrophenol; ONPG, *o*-nitrophenyl β-D-galactoside; pNP, *p*-nitrophenol; PNPG, *p*-nitrophenyl β-D-galactoside; TES, *N*-[tris(hydroxymethyl)methyl]-2-aminoethanesulfonic acid.

10.1021/bi035506j CCC: $25.00
Published on Web 11/01/2003

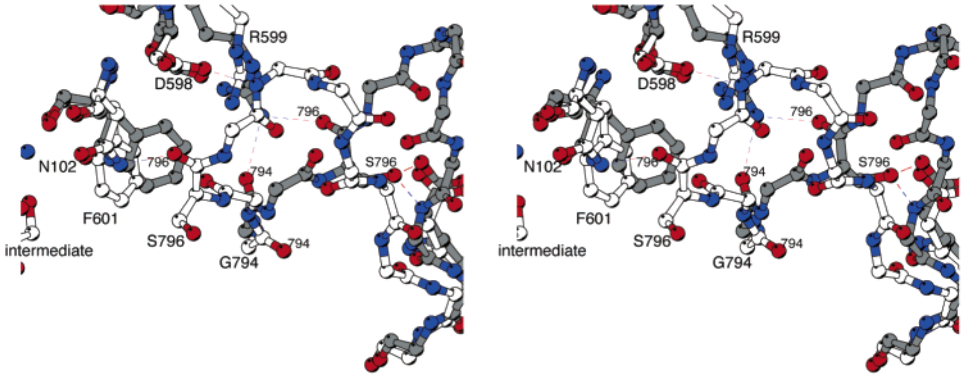

FIGURE 1: Stereoview showing the conformational switch correlated with deep-mode binding. The native, or open, conformation is shown with gray carbons and the intermediate, or closed, conformation is shown with carbons in white. In the open conformation Phe601 stabilizes Arg599, which in turn hydrogen-bonds to the backbone carbonyls of Gly794 and Ser796. As the substrate moves to the intermediate conformation these interactions are disrupted. Phe601 moves to the left and the 794−803 loop swings in the same direction toward the active site, making two new hydrogen bonds to Asn102 and Asp598. The Ser796 side chain, which was involved in an intraloop hydrogen bond in the open conformation (on the right) moves about 9 Å with its α- and *β*-carbons packing on Phe601.

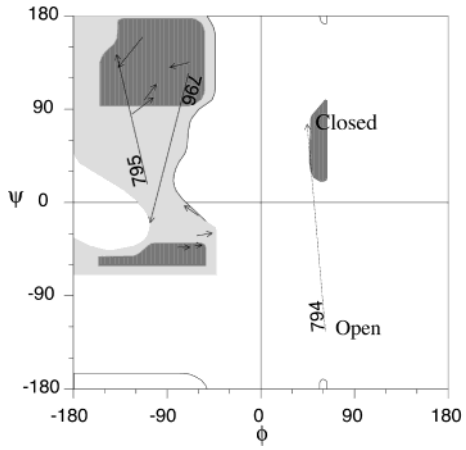

FIGURE 2: Ramachandran plot showing the changes in conformation of residues 794−803 in going from the open to the closed conformation. In the open configuration, Gly794 is in the lower right, a region that has relatively high energy for a nonglycine residue. In the closed configuration, Gly794 moves to a more allowed region of the plot. The four short arrows in the α-helical region indicate modest changes in conformation for residues 797, 800, 801, and 802. The short arrows in the extended region correspond to residues 798, 799, and 803. The figure was prepared with dphipsi (*27*).

(*13*, *18*). When the loop is in the native (open) conformation, Gly794 is in a region of the Ramachandran plot that would be high energy for a nonglycine residue, but it moves to a lower energy conformation (for nonglycine) in the ligand bound (closed) conformation (Figure 2). This suggests that a substitution at position 794 might force the loop into the closed conformation without a ligand present. To test this, Gly794 was replaced by an alanine. The structure and kinetic behavior were analyzed to gain insight into the role of the loop and of Gly794 in the action of *β*-galactosidase.

MATERIALS AND METHODS

Reagents and Buffers. 2-Amino-D-galactose, L-arabinose, D-xylose, D-lyxose, L-ribose, D-mannose, D-galactose, D-galactonolactone, lactose, TES, ONPG, PNPG, PETG, and IPTG were purchased from Sigma. Poly(ethylene glycol) [PEG] 8000 was from Hampton Research (Laguna Niguel, CA). Other reagents were obtained from Fisher or similar sources, and the purest grades of each of the chemicals used were purchased. TES assay buffer (pH 7.0) was formulated with 30 mM TES, 150 mM NaCl, and 1 mM $MgSO_4$.

Enzymes. G794A-*β*-Galactosidase was made with the Stratagene Quick-Change kit using the following oligonucleotide (and its complement): 5′-GCTGGATAACGACAT-TGCCGTAAGTGAAGCGACC-3′. The altered gene (the altered codon is underlined) was sequenced across the mutation site. The template used is a variant of *lacZ* that has an eight-residue substitution at the N-terminus (*12*). This change has no effect on the activity. Purification was done as previously reported for native enzyme (*12*).

Sodium Dodecyl Sulfate−Polyacrylamide Gel Electrophoresis. Analysis of the purity of the protein was done on Pharmacia's PhastSystem SDS−PAGE. Only enzyme that was >97% pure was used for kinetic analysis.

Assays. Appropriately diluted enzyme (50 *μ*L) was added to 950 *μ*L of TES assay buffer containing either ONPG or PNPG in 1.5 mL cuvettes. For routine assay, the ONPG or PNPG concentration was 6 mM. Assays to determine the values of the kinetic constants (k_{cat}, apparent k_{cat}, K_m, apparent K_m, and K_i) were done at 12 different substrate concentrations (six above the K_m and six below). The absorbance changes were measured at 420 nm (25 °C) on a Shimadzu UV 2101PC spectrophotometer with Shimadzu Kinetics software (version 2.0). Quantitation of the amount of nitrophenolate ion produced (pH 7.0) per minute was determined with the following extinction coefficients: ϵ_{420}(oNP) = 6.67 mM^{-1} cm^{-1} and ϵ_{420}(pNP) = 2.65 mM^{-1} cm^{-1}.

The production of glucose, galactose, and allolactose during lactose hydrolysis were monitored by a CE-based assay as previously described (*18*, *19*). Briefly, a solution of 0.375 M lactose in 50 mM Na_2HPO_4, 1 mM $MgCl_2$, and 250 nM *β*-galactosidase was allowed to react at room temperature. Samples (30 *μ*L) were removed at various times and the reactions were stopped by adding 60 *μ*L of 10% acetate in methanol and transferring to 60 °C. After samples were accumulated for about 24 h, each aliquot was derivatized by adding 30 *μ*L of derivatizing solution [1% (w/v) of $NaBH_3CN$ in ABEE stock solution, which is 10% (w/v) ethyl 4-aminobenzoate and 10% acetate in methanol] and heating at 70 °C for ∼30 min. This adds a charged aromatic ring to the reducing end of the sugar, allowing it to migrate in an electric field and to be monitored with absorption spectros-

Scheme 1: Postulated Reactions of β-Galactosidase in the Presence of an Inhibitor/Acceptor[a]

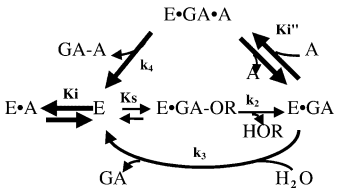

[a] The inhibitor/acceptor binds to both the free and the "galactosylated" enzyme. When bound to the galactosylated enzyme, the inhibitor/acceptor can react (k_4) to form galactosyl adducts. The solid lines represent reaction in the absence of inhibitor/acceptor while the shaded lines represent the extra reactions taking place when inhibitor/acceptor is added. The dots indicate that some sort of complex exists with the enzyme. E, β-galactosidase; GA-OR, β-galactosyl substrate; GA, galactose; HOR, aglycon product; A, inhibitor (acceptor); GA-A, galactosyl−inhibitor adduct. The step with k_2 as the rate constant is called "galactosylation" while the step with k_3 as the rate constant is called "degalactosylation".

copy at 306 nm. The derivatized sugars were extracted with 300/300 μL chloroform/water and centrifuged for 5 min. They were then separated by CE with a 23 mm capillary at 50−100 μA in a lithium borate buffer (pH 10.5). Galactose, glucose, and lactose standards were used to identify those peaks. Allolactose standards were created by separating reaction products from native enzyme acting on lactose with a gel-filtration column and analyzing with mass spectrometry (the mass was identical with lactose) and thin-layer chromatography [the allolactose ran slower than lactose (*20*)].

Kinetic Data Analysis. Kinetic constants were determined by nonlinear regression with Prism III software. The probable mechanism of β-galactosidase with inhibitor/acceptor present is shown in Scheme 1. Molecules that are competitive inhibitors are usually also acceptors (designated as A). These acceptors react (k_4) to form galactosyl−acceptor adducts (GA-A). Because the inhibitors are also acceptors, it is necessary to take this into account and this is done by (*21, 22*)

$$\frac{K_{m,app}}{k_{cat,app}} = \frac{K_m}{k_{cat}}\left[1 + \frac{[A]}{K_i}\right] \quad (1)$$

Experiments at different fixed concentrations of inhibitor (acceptor) were carried out and the K_i values obtained at the different concentrations were averaged. The value $k_{cat,app}/K_{m,app}$ is the ratio of k_{cat} to K_m in the presence of inhibitor.

The effects of acceptor binding on $k_{cat,app}$ are described by (*21*)

$$k_{cat,app} = \frac{k_{cat,app} - k_{cat}}{[A]}\frac{(k_2 + k_3)}{(k_2 + k_4)}K_i'' + \frac{k_2 k_4}{(k_2 + k_4)} \quad (2)$$

This equation gives a straight line when $k_{cat,app}$ is plotted against $(k_{cat,app} - k_{cat})/[A]$. The slope of the line is equal to $(k_2 + k_3)K_i''/(k_2 + k_4)$. If k_4 is less than k_3 (that is, if the reaction with acceptor is slow), the slope is larger than K_i'', and vice versa. The value of the intercept (the apparent k_{cat} of the reaction at infinite acceptor concentration) is equal to $k_2k_4/(k_2 + k_4)$. Since k_2 and k_4 are positive, it is always true that k_2 and k_4 are each equal to or greater than the intercept $k_2k_4/(k_2 + k_4)$. If k_4 is very large compared to k_2, the intercept value is essentially equal to k_2. The k_{cat} value for the reaction in the absence of acceptor is $k_2k_3/(k_2 + k_3)$. Again, both k_2 and k_3 are by definition equal to or greater than k_{cat}. It follows that if the intercept in the presence of acceptor is significantly larger than k_{cat}, then k_2 is much larger than k_3 and therefore k_{cat} is essentially equal to k_3.

Table 1: X-ray Data Collection and Refinement Statistics[a]

	G794A	G794A with IPTG
resolution (Å)	1.60	1.60
R_{merge} (%)	4.8 (30.0)	5.6 (27.3)
$\langle I\rangle/\langle\sigma(I)\rangle$	22.6 (3.3)	18.1 (3.0)
completeness (%)	92.1 (81.8)	94.8 (90.0)
redundancy	3.5	3.2
cell parameters		
a (Å)	149.7	149.5
b (Å)	168.6	168.3
c (Å)	201.0	200.4
R-factor (%)	19.2	18.7
R_{free} (%)	24.3	23.9
RMS deviations from ideal values		
bond lengths (Å)	0.017	0.016
bond angles (deg)	2.83	2.80
B-factor correlations (Å^2)	5.3	5.1
PDB code	1PX3	1PX4

a Numbers in parentheses refer to the highest resolution bin.

Crystallography. Crystals were grown in space group $P2_12_12_1$ as previously described (*12*). Diffraction data were collected at the Advanced Light Source, beamline 5.0.2, at ~100 K with 30% (v/v) dimethyl sulfoxide (DMSO) as the cryoprotectant. Data were processed with Denzo-Scalepack (*23*). Refinement was done with TNT (*24*), with native β-galactosidase as a starting model (PDB code 1DPO). Initial rigid-body refinement was followed with positional and *B*-factor refinement by use of the correlated *B*-factor restraint library in TNT. Several rounds of solvent addition and removal with Arp (*25*) were then alternated with positional and *B*-factor refinement. Several rounds of model building alternating with more refinement resulted in the final model. Coordinates and structure factors have been deposited in the Protein Data Bank (accession codes 1PX3 and 1PX4).

RESULTS

Structure of the Mutant. Table 1 shows data collection and refinement statistics for the G794A variant with and without IPTG bound. Both structures were determined to 1.6 Å resolution and refined to an *R*-factor below 20% (R_{free} below 25%) with reasonable deviations in bond lengths, angles, and other parameters from a small-molecule database. Excluding the 794−803 loop, both structures are very similar to native β-galactosidase. Root-mean-square deviations in main-chain atom positions after overlaying the structures on the native enzyme are 0.2 Å in both cases. The active-site Mg^{2+} and Na^+ ions are intact in both structures.

Figure 1 shows the conformational switch often induced by ligand binding in the deep mode. In the open conformation, the 794−803 loop is positioned somewhat away from the active site. Arg599, buttressed by Phe601, makes hydrogen bonds to backbone carbonyls within the loop. In the closed conformation, Phe601 swings into a different rotamer and Arg599 becomes disordered. The 794−803 loop swings toward the active site with Ser796 packing on Phe601, and new hydrogen bonds are created from the loop to the side chains of Asn102 and Asp598.

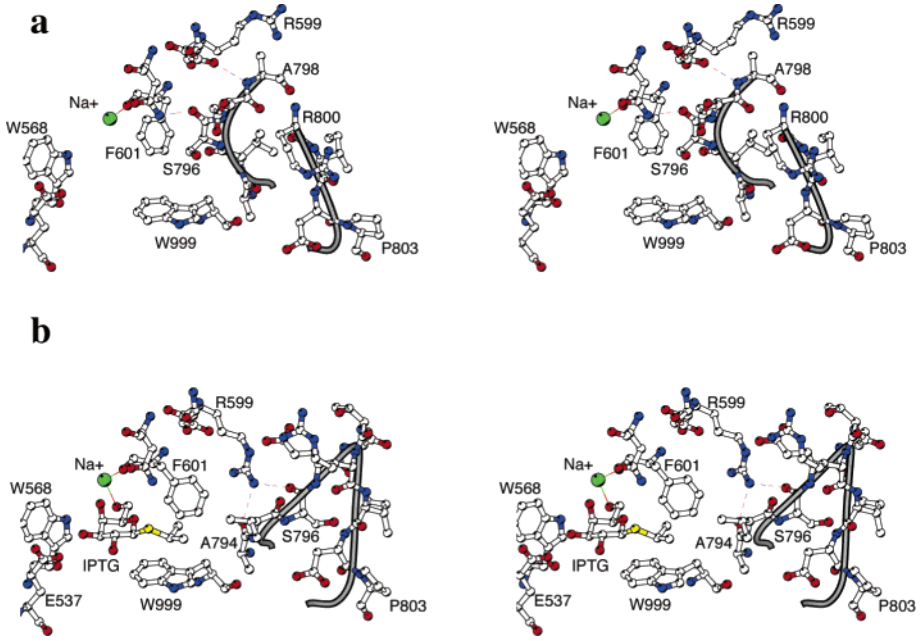

FIGURE 3: Stereoview showing the active-site region of the refined structure of G794A. (a) The backbone of the 794−803 loop is highlighted. In contrast to wild type, the mutant adopts the closed conformation. (b) Structure of the active-site region of mutant G794A with IPTG bound. In this case the 794−803 loop has the open conformation, similar to wild type with IPTG bound.

Table 2: Kinetic Constants for Wild Type and G794A-β-Galactosidase

	k_{cat}(ONPG) (s^{-1})	k_{cat}(PNPG) (s^{-1})	K_m(ONPG) (mM)	K_m(PNPG) (mM)
wild type	600 ± 11	90 ± 1	0.12 ± 0.01	0.040 ± 0.002
G794A	189 ± 10	111 ± 4	0.19 ± 0.02	0.24 ± 0.03

Table 3: Competitive Inhibition of Wild Type and G794A-β-Galactosidase[a]

inhibitor	K_i for wild type (mM)	K_i for G794A (mM)
IPTG	0.11	0.59
PETG	0.001	0.006
D-galactose	24	8
lactose	1.2	1.0
D-lyxose	80	31
2-amino-D-galactose	1.9	1.0
D-galactonolactone	0.70	0.034
L-ribose	0.24	0.021
D-glucose	>400	19
L-arabinose	220	220

[a] The standard errors are less than 10% in each case. When the K_i values were large (greater than 400 mM), accurate K_i values could not be obtained because even the addition of large amounts of inhibitor had very small effects on the rates.

In contrast to wild type, the G794A-β-galactosidase structure is similar to the closed conformation described above (Figure 3a). Phe601 and Arg599 are both in their closed conformations. Some of the 794−803 loop is disordered (residues 798−801, depending on the chain) but those that are visible are clearly in the closed conformation. The structure of G794A with IPTG bound, however, shows that the enzyme is in its open conformation (i.e., similar to wild type with IPTG bound) (Figure 3b). Phe601 is in the native conformation, packing with Arg599, which hydrogen-bonds to the 793−804 loop. The loop is better ordered than in the absence of IPTG, with all residues visible.

Several attempts were made to determine the structure of complexes between the enzyme and glucose. The native enzyme and G794A were tested, both with and without a trapped covalent intermediate. Additionally, a glucose variant, 3-*O*-methylglucose, which binds better to the intermediate, was tried (*22*). Although in some cases weak electron density could be seen adjacent to Trp999, a convincing model could not be refined. Information about glucose binding can, however, be determined from the kinetic data (see below).

Kinetic Constants. Table 2 compares the k_{cat} and K_m values for wild-type β-galactosidase and G794A-β-galactosidase with ONPG and PNPG. The k_{cat} values with G794A-β-galactosidase decreased for ONPG but increased for PNPG. The K_m values for G794A-β-galactosidase with the two substrates were roughly equal but both were larger than those for wild type (especially PNPG).

Inhibition. Table 3 lists the inhibition constants obtained for a series of inhibitors. Values greater than 400 mM are not presented. In those cases even the addition of large amounts of inhibitor gave such poor inhibition that the values calculated were deemed to be inaccurate. IPTG and PETG inhibited G794A-β-galactosidase severalfold more poorly than they inhibited wild type, while D-galactose, D-lyxose, and 2-amino-D-galactose inhibited G794A-β-galactosidase 2−3-fold better. The two transition-state analogues tested, D-galactonolactone and L-ribose, were especially good inhibitors. Relative to wild type, D-glucose was also a very good inhibitor of G794A-β-galactosidase.

Transgalactosidic Reactions. The effects of adding methanol were plotted by use of eq 2 and are shown in Figure 4. The intercept for G794A-β-galactosidase was more than 7.5-fold greater than the k_{cat} for ONPG but about 2× greater with PNPG. Glucose caused the rates to decrease (Figure 5). The intercept value obtained for wild-type β-galactosidase with ONPG and glucose is 230 s^{-1}. The intercept values with ONPG and PNPG for G794A-β-galactosidase were very small (5.5 s^{-1}). Since this is much smaller than the k_2 value, it is equivalent to k_4 and thus the reaction to form adducts (allolactose) is very slow. The slopes were also smaller. The

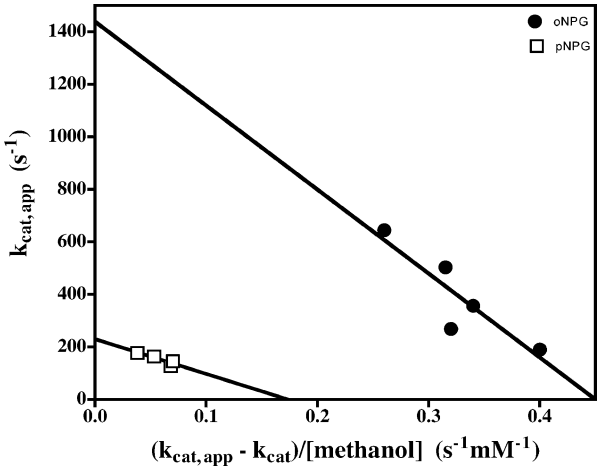

FIGURE 4: Plot of the effects of methanol on the activity of G794A-β-galactosidase with ONPG and PNPG, based on eq2. (●) ONPG; (□) PNPG.

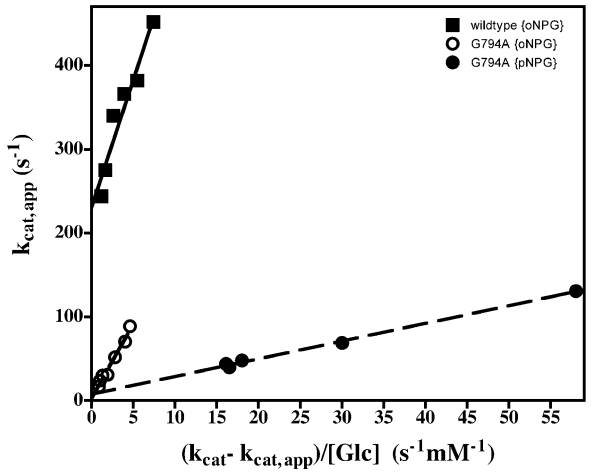

FIGURE 5: Plot of the effects of glucose on the activity of wild-type β-galactosidase with ONPG and of G794A-β-galactosidase with ONPG and PNPG, based on eq 2. (■) Wild type with ONPG; (●) G794-β-galactosidase with PNPG; (○) G794A-β-galactosidase with ONPG.

calculated K_i'' (Scheme 1) for wild-type β-galactosidase is 17 mM, while the average of the two K_i'' values obtained with ONPG and PNPG for glucose was 3 mM for G794A-β-galactosidase.

Allolactose. Allolactose formation was studied by CE (data not shown). As expected from the above results, G794-β-galactosidase formed a significantly lower (about 3-fold) transient level of allolactose than did wild-type β-galactosidase.

DISCUSSION

Altered Inhibition and the Energetics of the Conformational Switch. In the absence of active-site ligands, the native enzyme adopts the open conformation, while G794A-β-galactosidase has the closed conformation. The structures show that IPTG binds to the open conformation in both cases. Thus IPTG binding to G794A-β-galactosidase stabilizes the open conformation. Since the closed conformation is the favored form, this costs free energy and consequently IPTG binds more poorly to G794A-β-galactosidase than to wild-type enzyme. A similar argument can be made for the binding of D-galactonolactone and L-ribose, except that they bind to the closed conformation rather than the open. They thus bind more tightly to G794A-β-galactosidase than to the native enzyme because in the latter case some of the binding energy is used to effect the conformational switch. This energy is not needed with G794A-β-galactosidase.

Because the inhibitor binds to the same conformation of both wild type and G794A-β-galactosidase, the difference in binding affinity between the two enzymes ($\Delta\Delta G_{binding}$) can be used to estimate the free energy difference between the open and closed conformations as follows:

$$\Delta G(\text{open} \leftrightarrow \text{closed}) \cong \Delta\Delta G_{binding} = RT \ln\left(\frac{K_i^{G794A}}{K_i^{native}}\right) \quad (3)$$

Using the values from Table 3 for IPTG, we calculate a free energy difference between the two conformations of about 1 kcal/mol. If the values for binding D-galactonolactone and L-ribose are used, the value is between 1.5 and 2.0 kcal/mol. These values suggest that it is more difficult to close the native enzyme than to open G794A. This is consistent with the crystallography, which shows closed conformations to be somewhat more disordered than open ones. Both transitions, however, would be quite accessible to thermal fluctuations.

The above discussion appears to be consistent with the behavior of other ligands. On the basis of its structure, we predict that PETG would bind to the open conformation, and the inhibition data show that it binds to wild-type enzyme better than to G794A-β-galactosidase. D-Galactose, D-lyxose, L-ribose, and D-galactonolactone all bind in the deep mode (*13*; D.H.J. and B.W.M., unpublished results) and the inhibition data show that they all bind better to G794A-β-galactosidase. Of these, L-ribose and D-galactonolactone both trigger the conformational change to the closed form and they bind 11- and 20-fold better, respectively, to G794A-β-galactosidase. D-Galactose and D-lyxose, which both bind deeply but do not trigger the conformational change, only bind about 2−3-fold better to G794A-β-galactosidase than to the wild-type enzyme.

The relatively good binding of glucose to the free enzyme (Table 3) indicates that the closing of the loop induced by the substitution of an Ala for Gly794 also creates a preformed site for glucose to bind. It is likely that the glucose binds at the acceptor site of the free enzyme in this case. The binding site for the acceptor is normally created upon cleavage of the glycosidic bond and is thought to be a consequence of a conformational change. For the substituted enzyme, the free enzyme already has a closed conformation and thus, presumably, a preformed acceptor site.

Kinetics. The intercepts of the ONPG and PNPG plots with methanol (Figure 4) were 1440 and 230 s^{-1}, respectively. It will be shown below that k_4 for methanol is very large and thus the intercept of the PNPG plot (230 s^{-1}) is essentially equal to the k_2 value for PNPG. Since the k_{cat} [$=k_2k_3/(k_2 + k_3)$] for PNPG is 111 s^{-1} and k_2 is 230 s^{-1}, k_3 is equal to 214 s^{-1}. If one then uses this k_3 value (which is common for both substrates) and the k_{cat} value for ONPG (189 s^{-1}), the k_2 value for ONPG is 1620 s^{-1}. This is only a little higher than the intercept of the plot with methanol and ONPG and it follows that k_4 for methanol is much larger than the k_2 values of PNPG and ONPG. Since the ONPG k_{cat} (in the

Table 4: Summary of the Rate Constants and K_s Values for Wild Type and G794A-β-Galactosidase

	k_3(G794A) (s^{-1})	k_3(wt) (s^{-1})	k_2(G794A) (s^{-1})	k_2(wt) (s^{-1})	K_s(G794A) (mM)	K_s(wt) (mM)
ONPG	214	1000	1620	1500	1.6	0.33
PNPG	214	1000	230	90	0.51	0.04

absence of methanol) is much smaller than the intercept of the plot with methanol and ONPG (Figure 4), the k_{cat} for ONPG must approximate the k_3 value and thus k_3 is approximately equal to 189 s^{-1}. This is not very different from the value of 214 s^{-1} calculated above and shows that the values obtained are reliable. The data show that substitution of an Ala for Gly794 cause the k_3 value to decrease (from 1000 s^{-1} for wild type to 214 s^{-1}) while the value of k_2 increases about 2.5-fold relative to wild type with PNPG and increases from 1500 to 1620 s^{-1} with ONPG. This is similar to results for other substitutions at Gly794, in which k_3 decreased and k_2 increased (*17*). One can use the values of k_2, k_3, and K_m and the equation for K_m [$=k_3K_s/(k_2 + k_3)$] to calculate K_s values for ONPG and PNPG. The K_s value obtained for ONPG is 1.6 mM (the wild-type K_s is 0.33 mM) and the K_s for PNPG is 0.51 mM (the wild-type K_s is 0.04 mM). This information is summarized in Table 4. Thus, the substitution of Gly794 by alanine causes the substrates to bind more poorly. This binding is to the open form of the enzyme and thus requires more energy for the mutant than for wild type. This is similar to results for other substitutions at position 794 (*17*). Substrate binding is destabilized by a larger factor for PNPG than for ONPG.

To summarize the kinetic results, the variants at position 794 bind substrates more poorly, carry out the galactosylation step more rapidly for poorer substrates, and perform degalactosylation more slowly than the wild-type enzyme.

Basis for Changes in Activity. Together, the structural and kinetic data offer an explanation for the increased activity of Gly794 variants against PNPG and lactose (*17*). By favoring the closed conformation, the G794A mutation moves the enzyme further along the reaction coordinate than native enzyme. This destabilizes the ground state toward the transition state for the first step of the reaction. Binding of the transition-state analogues is stabilized considerably, while substrate binding is destabilized. Thus, one would expect changes in k_2. It should be remembered, however, that transition-state analogues are not perfect representations of the transition state and the stabilization of the actual transition state may not be as great as for the transition-state analogue inhibitors. For ONPG the k_2 value increases by a small amount. For PNPG, it increases about 2.5-fold. The differences are probably due to the different degrees of destabilization of the two substrates (note that the K_s of PNPG is about 13 times larger than for wild type, while the K_s of ONPG is only about 5 times larger).

The structures suggest that G794A-β-galactosidase should also stabilize the intermediate. Because the rate of degalactosylation decreases significantly, the variants must stabilize the intermediate more than the second transition state and thus more activation energy is required for k_3 with G794A-β-galactosidase than with wild type. If one compares the k_3 values for wild type and G794A-β-galactosidase, the difference in stabilization between wild type and G794A-β-galactosidase is about 1 kcal/mol.

Effect of Glucose as an Acceptor. The K_i'' for glucose with G794A-β-galactosidase is severalfold smaller than the K_i'' of wild type. This suggests that the acceptor binding site is thus more complementary to the structure of glucose with this form of the enzyme. When an Ala replaces Gly794, the loop must cause the residues that bind glucose to be positioned a little differently so that binding is better. However, the closing of the loop and the tighter binding upon substituting Ala for Gly794 must draw the glucose out of a reactive position as the reaction is very slow (5.5 s^{-1}) compared to wild type (230 s^{-1}). Another reason for the lower activity could be that the transition state is bound differently (attested by the better inhibition by transition-state analogues) and is no longer positioned ideally for attack by glucose.

The lower transglycosylation activity of G794A contrasts with recent experiments designed to improve the ability of β-galactosidase to make β-(1,6) linkages as an alternative to synthetic organic chemistry (*26*). Here, the nucleophile, Glu537, was changed to a serine. This variant has drastically reduced hydrolytic activity but will perform transglycosylation on α-galactosyl fluoride and various glucosyl acceptor molecules to form β-(1,6) linkages between galactose and glucose. In contrast to the effect of G794A on wild-type enzyme, the G794D mutation increased the transglycosylation activity of E537S enzyme. Possibly the side chain at position 794 is involved in positioning the acceptor molecule, or transglycosylation by E537S uses a different catalytic mechanism than native enzyme. Further investigation will be required to understand these differences.

If mutations exist that increase the hydrolytic activity against the natural substrate lactose, why are they not utilized in nature? A possible answer lies in the transglycosylation activity of β-galactosidase. Normal β-galactosidase has two important functions for *E. coli*. First is its hydrolytic activity, which results in the cleavage of lactose to galactose and glucose and subsequently to ATP synthesis. Second, and equally important, is the production of allolactose, the inducer for the lac operon. Without this second activity, little enzyme is produced. The reduced ability of the mutated enzyme to make the inducer, allolactose, explains its absence in the cell.

ACKNOWLEDGMENT

We thank Jon Wray for very helpful discussions and Leslie Gay for expert technical assistance. X-ray data were collected at the Advanced Light Source.

REFERENCES

1. Jacob, F., and Monod, J. (1961) *J. Mol. Biol. 3*, 318−356.
2. Beckwith, J. R., and Zipser, D. (1970) *The Lactose Operon*, Cold Spring Harbor Laboratory Press, Cold Spring Harbor, NY.
3. Miller, J. H., and Reznikoff, W. S. (1980) *The Operon*, Cold Spring Harbor Laboratory Press, Cold Spring Harbor, NY.
4. Müller-Hill, B. (1996) *The lac Operon*, Walter de Gruyter, New York.
5. Fowler, A., and Zabin, I. (1978) *J. Biol. Chem. 253*, 5521−5525.
6. Kalnins, A., Otto, K., Ruther, U., and Müller-Hill, B. (1983) *EMBO J. 2*, 593−597.
7. Cohn, M. (1957) *Bacteriol. Rev. 21*, 140−168.
8. Case, G. S., Sinnott, M. L., and Tenu, J. P. (1973) *Biochem. J. 133*, 99−104.
9. Huber, R. E., Parfett, C., Woulfe-Flanagan, H., and Thompson, D. J. (1979) *Biochemistry 18*, 4090−4095.

10. Tenu, J. P., Viratelle, O. M., and Yon, J. (1972) *Eur. J. Biochem. 26*, 112−118.
11. Jacobson, R. H., Zhang, X.-J., DuBose, R. F., and Matthews, B. W. (1994) *Nature 369*, 761−766.
12. Juers, D. H., Jacobson, R. H., Wigley, D., Zhang, X.-J., Huber, R. E., Tronrud, D. E., and Matthews, B. W. (2000) *Protein Sci. 9*, 1685−1699.
13. Juers, D. H., Heightman, T., Vasella, A., McCarter, J., Mackenzie, L., Withers, S. G., and Matthews, B. W. (2001) *Biochemistry 40*, 14781−14794.
14. Huber, R. E., Kurz, G., and Wallenfels, K. (1976) *Biochemistry 15*, 1994−2001.
15. Huber, R. E., Hakda, S., Cheng, C., Cupples, C. G., and Edwards, R. A. (2003) *Biochemistry 42*, 1796−1803.
16. Martinez-Bilbao, M., Holdsworth, R. E., Edwards, L. A., and Huber, R. E. (1991) *J. Biol. Chem. 266*, 4979−4986.
17. Martinez-Bilbao, M., and Huber, R. E. (1994) *Biochem. Cell. Biol. 72*, 313−319.
18. Juers, D. H. (2000) Ph.D. Thesis, University of Oregon, Eugene, OR, p 211.
19. Zeleny, R., Altman, F., and Praznik, W. (1997) *Anal. Biochem. 246*, 96−101.
20. Burstein, C., Cohn, M., Kepes, A., and Monod, J. (1965) *Biochim. Biophys. Acta 95*, 634−639.
21. Deschavanne, P. J., Viratelle, O. M., and Yon, J. M. (1978) *J. Biol. Chem. 253*, 833−837.
22. Huber, R. E., Gaunt, M. T., and Hurlburt, K. L. (1984) *Arch. Biochem. Biophys. 234*, 151−160.
23. Otwinowski, Z., and Minor, W. (1997) in *Macromolecular Crystallography, Part A* (Carter, C. W., and Sweet, R. M., Eds.) pp 307−326, Academic Press, San Diego, CA.
24. Tronrud, D. (1997) *Methods Enzymol. 277*, 306−319.
25. Lamzin, V., and Wilson, K. (1993) *Acta Crystallogr. D49*, 129−147.
26. Jakeman, D. L., and Withers, S. G. (2002) *Can. J. Chem. 80*, 866−870.
27. Quillin, M. L. (1995) Ph.D. Thesis, Rice University, Houston, TX.

BI035506J